Structural and Spectral Response of Green Fluorescent Protein Variants to Changes in pH[†,‡]

Marc-André Elsliger, Rebekka M. Wachter, George T. Hanson, Karen Kallio, and S. James Remington*

Institute of Molecular Biology and Department of Physics, University of Oregon, Eugene, Oregon 97403

Received January 28, 1999; Revised Manuscript Received March 9, 1999

ABSTRACT: The green fluorescent protein (GFP) from the jellyfish *Aequorea victoria* has become a useful tool in molecular and cell biology. Recently, it has been found that the fluorescence spectra of most mutants of GFP respond rapidly and reversibly to pH variations, making them useful as probes of intracellular pH. To explore the structural basis for the titration behavior of the popular GFP S65T variant, we determined high-resolution crystal structures at pH 8.0 and 4.6. The structures revealed changes in the hydrogen bond pattern with the chromophore, suggesting that the pH sensitivity derives from protonation of the chromophore phenolate. Mutations were designed in yellow fluorescent protein (S65G/V68L/S72A/T203Y) to change the solvent accessibility (H148G) and to modify polar groups (H148Q, E222Q) near the chromophore. pH titrations of these variants indicate that the chromophore pK_a can be modulated over a broad range from 6 to 8, allowing for pH determination from pH 5 to pH 9. Finally, mutagenesis was used to raise the pK_a from 6.0 (S65T) to 7.8 (S65T/H148D). Unlike other variants, S65T/H148D exhibits two pH-dependent excitation peaks for green fluorescence with a clean isosbestic point. This raises the interesting possibility of using fluorescence at this isosbestic point as an internal reference. Practical real time in vivo applications in cell and developmental biology are proposed.

The green fluorescent protein (GFP)[1] from the jellyfish *Aequorea victoria* has been used extensively in molecular and cell biology as a genetically encoded marker. It generates its own fluorophore in an autocatalytic fashion by the spontaneous cyclization and oxidation of the internal -Ser65-Tyr66-Gly67- sequence (*1*). The overall fold of the protein consists of an unusual 11-stranded β-barrel that contains a coaxial helix in its center from which the fluorophore is generated (*2*−*4*). A large number of mutants have been identified that exhibit broadly varying absorption and emission properties (*1*, *5*). Some exhibit enhancement of emission intensity, such as the S65T variant (*6*), with fluorescence occurring at similar wavelengths as in wild type (WT). Others exhibit significant spectral shifts, such as the yellow fluorescent proteins (YFPs) that have the longest wavelength emissions of all engineered GFPs (*2*, *7*).

Many applications of GFP in physiological studies of living cells have been described in recent reviews (*8*−*11*). Some time ago, we proposed a novel application that involves the use of blue fluorescent protein (BFP) as a reporter of the pH within cellular compartments (*12*). The significant pH dependence of BFP fluorescence intensity between pH 5 and pH 7, accompanied by a small shift in peak wavelength, appeared promising for this type of application. This has, in part, prompted recent studies describing the pH sensitivity of other GFP variants (*7*, *13*−*16*) and the use of these variants as noninvasive intracellular pH indicators. Kneen and co-workers employed S65T/F64L to determine the pH of the cytoplasm of CHO and LLC-PK1 cell cultures. Since a pK_a around 6, as for S65T, is too low to measure the pH of alkaline organelles, Llopis and co-workers used a YFP variant with a pK_a of 7.1 to measure the pH of mitochondria, the cytosol, and the Golgi, in HeLa cells and in rat neonatal cardiomyocytes.

Though WT is relatively insensitive to changes in pH (*17*), the two absorbance bands of a number of engineered GFPs, the UV band A and the visible band B, are interconvertible as a function of pH and are thought to be due to differing protonation states of the chromophore (*13*). The π-system of the chromophore contains, in principle, two titratable groups, the hydroxyl at the phenolic end and the imidazolinone ring nitrogen of the heterocyclic end (Scheme 1). On the basis of the spectrophotometric titrations carried out on the unfolded WT protein (*18*) and studies on the enzymatically digested protein and the synthesized chromophore (*19*), it is generally believed that band A corresponds to the neutral and band B to the anionic form of the chromophore. Nevertheless, the relevance of the charge states in solution to the charge states in the intact protein has not yet been established, and the protonation state of the heterocyclic ring nitrogen has not yet been determined.

The YFPs have a T203Y substitution which is responsible for the red-shifted emission at 528 nm and the additional

[†] This work was supported in part by grants from the National Science Foundation (MCB 9728162) to S.J.R., a Fonds de la Recherche en Santé du Quebec fellowship (980457-103) to M.-A.E., and a National Institutes of Health postdoctoral fellowship (1 F32 GM19075-01) to R.M.W.

[‡] The coordinates for GFP S65T at pH 8.0 and 4.6 have been deposited in the Brookhaven Protein Data Bank with accession codes 1emg and BNL-26390, respectively.

* To whom correspondence should be addressed: phone (541) 346-5190; fax (541) 346-5870; e-mail jim@uoxray.uoregon.edu.

[1] Abbreviations: GFP, green fluoresecent protein; WT, wild-type GFP; YFP, yellow fluorescent protein; BFP, blue fluorescent protein.

10.1021/bi9902182 CCC: $18.00
Published on Web 04/10/1999

Scheme 1: Four Possible Charge States of the Chromophore[a]

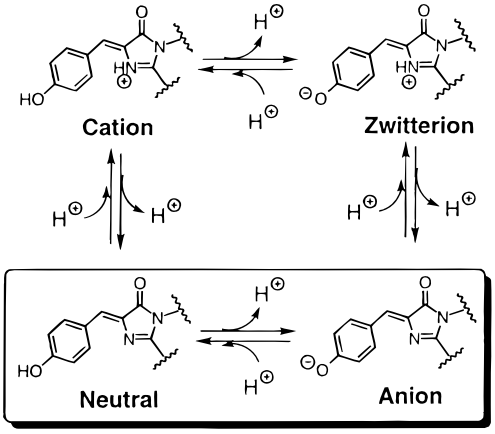

[a] The neutral and anionic states are likely the relevant states in the S65T and YFP variants.

substitutions S65G/V68L/S72A which have been shown to improve the protein's brightness in live cells (*20*). In the recently determined crystal structures of YFP and YFP H148G to 2.5 and 2.6 Å resolution, respectively, the introduced tyrosine in position 203 was found to be involved in a π-stacking interaction with the chromophore (*7*). As a consequence of the YFP H148G mutation, an invagination on the protein surface is formed that exposes the phenolic end of the chromophore to solvent (*7*).

We carried out crystallographic analyses of the mutant GFP S65T at both basic (pH 8.0) and acidic (pH 4.6) pH, identifying the phenolic end of the chromophore as the site of protonation, with the heterocyclic ring nitrogen most likely unprotonated. We carried out a mutational analysis of charged and polar groups adjacent to the chromophore in S65T and YFP background, with the goal of understanding the role of these residues in the titration behavior and of developing variants with altered pK_as that could be applied to a broad range of pH measurements.

MATERIALS AND METHODS

Structure Determination of GFP S65T at High and Low pH. GFP S65T was concentrated to 12 mg/mL in 20 mM Tris, pH 7.9. Flute-shaped crystals measuring 0.05 mm across and up to 1.0 mm long grew in hanging drops containing 5 μL of protein and 5 μL of mother liquor at room temperature. The high pH mother liquor contained 23−26% PEG 4000 at pH 8.0 in 50 mM HEPES and 50 mM $MgCl_2$. The low pH mother liquor contained 10−13% PEG 3400 at pH 4.6 in 100 mM sodium acetate and 100 mM ammonium acetate. Crystals grown at pH 8.0 were also equilibrated to pH 4.6 with low pH mother liquor. X-ray diffraction data were collected at room temperature using a Raxis-IV image plate mounted on a Rigaku RUH3 rotating anode generator equipped with mirrors. The three data sets were processed with Denzo v1.9 and scaled using ScalePack (*21*). The space group is $P2_12_12_1$, with unit cell parameters $a = 52.0$ Å, $b = 62.7$ Å, and $c = 69.9$ Å, essentially isomorphous to those originally described (*2*). The GFP S65T selenomethionine coordinate file 1ema.pdb (*2*) was used as a model for phasing. A model for the anionic chromophore was obtained by semiempirical molecular orbital calculations using AM1 in the program SPARTAN version 4.1 (Wavefunction Inc., Irvine, CA). This minimized structure, which was planar, compared very favorably with a related small molecule crystallographic structure (*22*) and also with the model used during refinement of GFP S65T, where a simpler modeling program had been employed (*2*).

Table 1: Data Collection and Atomic Model Statistics of GFP S65T at pH 8.0 and 4.6

	S65T		
	pH 8.0	pH 4.6	pH 8.0 → 4.6
total observations	93 073	63 981	72 081
unique reflections	16 011	12 440	8 499
completeness[a]	99	96	98
completeness (shell[b])	94	94	90
no. of crystals	1	1	1
R_{merge}[c] (%)	7.5	5.8	6.3
resolution	2.0	2.25	2.45
atomic model statistics			
space group	$P2_12_12_1$	$P2_12_12_1$	$P2_12_12_1$
molecules per asym. unit	1	1	1
crystallographic *R*-factor	0.190	0.190	0.204
protein atoms	1841	1841	1841
solvent atoms per asym unit	110	110	110
bond length deviations (Å)	0.009	0.009	0.009
bond angle deviations (deg)	2.12	2.18	1.82
thermal parameter restraints (Å^2)	3.87	3.81	2.75

[a] Completeness is the ratio of the number of observed $I > 0$ divided by the theoretically possible number of intensities. [b] Shell is the highest resolution shell (2.10−2.00 Å for pH 8.0, 2.34−2.25 Å for pH 4.6, and 2.55−2.45 for pH 8.0 → pH 4.6). [c] $R_{merge} = \sum|I_{hkl} - \langle I\rangle|/\sum\langle I\rangle$, where $\langle I\rangle$ = average of individual measurements of I_{hkl}.

Positional refinement was carried out using the data to 4.0 Å, then to 3.5 and 3.0 Å, and finally to the limit of resolution (Table 1), using the program TNT (*23*). Electron density maps ($2F_o - F_c$ and $F_o - F_c$) were inspected using O (*24*). *B*-factors were refined using the default TNT *B*-factor correlation library. B-factor correlation values derived from His and Phe were used to model the chromophore atoms.

Mutagenesis and Protein Preparation. GFP variants were prepared using the PCR-based QuikChange Site-Directed Mutagenesis Kit (Stratagene, La Jolla, CA), according to the manufacturer's directions. As a template, GFP S65T DNA and the original YFP mutation 10c were employed (*2*). The YFP template incorporates the mutations T203Y/S65G/V68L/S72A. Mutations were verified by sequencing the entire gene, and all GFP variants were expressed and purified as described (*2*).

pH Titrations of the GFP S65T and YFP Variants. pH titrations of S65T, S65T/H148D, YFP, YFP H148Q, YFP H148G, and YFP E222Q were carried out in 75 mM buffer and 140 mM NaCl. Appropriate buffers were selected from acetate, phosphate, Tris, or CHES, depending on the pH range of interest, and the pH was adjusted with HCl and NaOH. Small aliquots of 16 mg/mL protein (20 mM HEPES, pH 7.0, 0.2 μm filtered) were diluted 48-fold into the appropriate buffer and allowed to equilibrate for 5 min at room temperature. The absorbance was then scanned between 250 and 600 nm with a Shimadzu 2101 spectrophotometer at room temperature. The optical density of the long-wave band B was plotted as a function of pH and fitted to a titration curve (Kaleidagraph, Synergy Software). Reversibility of the spectral pH sensitivity was tested by adjusting the pH of the same protein sample repeatedly. As a control, a sample of YFP was diluted into 100 mM glycine, pH 2.5, which

Table 2: Chromophore pK_a of GFP Variants

variants	pK_a by absorbance	pK_a by fluorescence
S65T	5.95 (±0.02)	6.04 (±0.01)
S65T/H148D	7.95 (±0.02)	7.75 (±0.02)
YFP	7.00 (±0.03)	6.95 (±0.03)
YFP H148Q	7.58 (±0.02)	7.46 (±0.03)
YFP H148G	8.02 (±0.01)	7.93 (±0.04)
YFP E222Q	6.77[a] (±0.02)	6.95 (±0.03)

[a] This number is not as reliable as the other pK_a values measured by absorbance since the efficiency of chromophore formation was extremely poor for this mutant.

denatures the protein. The absorbance maximum was blue shifted to 380 nm, consistent with previous studies on unfolded GFPs (*18*).

Fluorescence measurements were carried out on a Hitachi F4500 fluorescence spectrophotometer at a protein concentration of approximately 0.01 mg/mL, in the same buffers used for absorbance measurements. For emission scans, the excitation wavelength was set to the absorbance maximum of the long-wave band B of the particular mutant (see Table 3), and the emission was scanned between 500 and 600 nm. Peak emission intensity was plotted as a function of pH and curve-fitted as above. For excitation scans, the excitation wavelength was scanned between 350 and 550 nm while monitoring emission intensity at 510 nm.

RESULTS AND DISCUSSION

X-ray Structures of S65T at High and Low pH and Assignment of Chromophore Protonation States. To identify titrating groups on the chromophore, we determined crystal structures of S65T at both pH 8.0 (PEG/HEPES) and pH 4.6 (PEG/acetate) to 2.0 and 2.25 Å resolution, respectively (Table 1). To confirm the interconversion of the two forms within the same crystal, the mother liquor of a crystal grown at pH 8.0 was exchanged with pH 4.6 mother liquor and the structure was determined to 2.4 Å resolution.

The S65T X-ray data at low and high pH clearly reveal structural changes consistent with titration of the phenolic hydroxyl only (Scheme 1). Figure 1 shows the electron density around the chromophore at high and low pH, whereas Figure 2 schematically details the structural changes and proposed hydrogen bonds. The side chain of Thr203 rotates around χ_1 by 100° upon acidification, breaking a hydrogen bond between the γ-hydroxyl and the chromophore phenolate hydroxyl and confirming protonation of the phenolic end of the chromophore. Furthermore, the hydrogen bond between His148 and the chromophore is lost at low pH, where His148 has moved away from the phenolate by 0.73 Å (the charge state of His148 is discussed in a later section). There is no structural evidence for titration of a second group on the chromophore, such as the imidazolinone ring nitrogen that is derived from the backbone nitrogen of Tyr66. No rearrangements are observed in close vicinity of this nitrogen. In particular, the carboxylate of Glu222 is in the same position in both high and low pH structures. The soaking experiment clearly establishes that the two structures are interconvertible. Lowering the pH from 8.0 to 4.6 in the crystal results in a structure identical to the one obtained when the crystal was grown at pH 4.6, albeit at a small loss of diffraction resolution (from 2.0 to 2.4 Å).

The findings presented here are consistent with a pK_a for the imidazolinone ring nitrogen (Scheme 1) well below 5. This confirms the conclusions by Niwa et al. (*19*) based on solution studies but does not support results based on theoretical calculations which suggested that this nitrogen is protonated (*25*). The crystallographic results support a model where the chromophore ground state of S65T consists of a pH-dependent equilibrium between the neutral and anionic forms, with the heterocyclic ring nitrogen deprotonated. This model is likely to hold for other variants as well but may not necessarily be applicable to all GFPs. Other chromophore protonation states could, in principle, be operative in some instances if there are changes in the hydrogen bond or charge configuration near the chromophore.

Modulation of the Chromophore Ionization Constant by Mutagenesis. Absorbance and fluorescence spectra of S65T and YFP exhibit a striking pH dependence (shown for YFP in Figure 3), consistent with recent reports on related variants (*13, 14*). To determine the influence of certain surrounding residues on chromophore pK_a, we studied a series of mutants in a S65T and a YFP background. His148 is directly hydrogen bonded to the phenolic end of the chromophore in the high pH S65T structure (Figure 2) and in YFP (*7*) and constitutes a barrier between the chromophore and bulk solvent. In GFP S65T, we replaced His148 with an aspartic acid to introduce a potential negative charge near the chromophore. In YFP, we replaced His148 with a glutamine to eliminate a titratable group and with a glycine to investigate the effects of rendering the chromophore accessible to solvent. We further replaced Glu222 with a glutamine

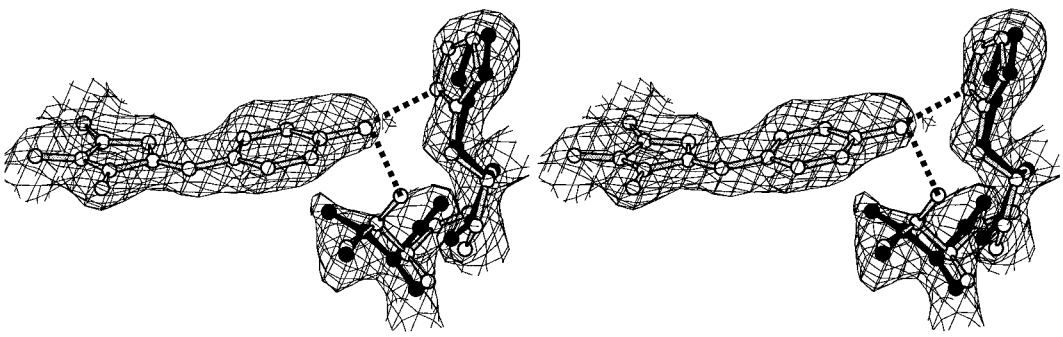

FIGURE 1: Stereoview of a portion of the $2F_o - F_c$ electron density map of S65T at pH 4.6, contoured at 1 standard deviation (black bonds). Overlayed is the model of the pH 8.0 crystal structure (gray bonds). Shown is the chromophore (same position in both models), Thr203, and His148.

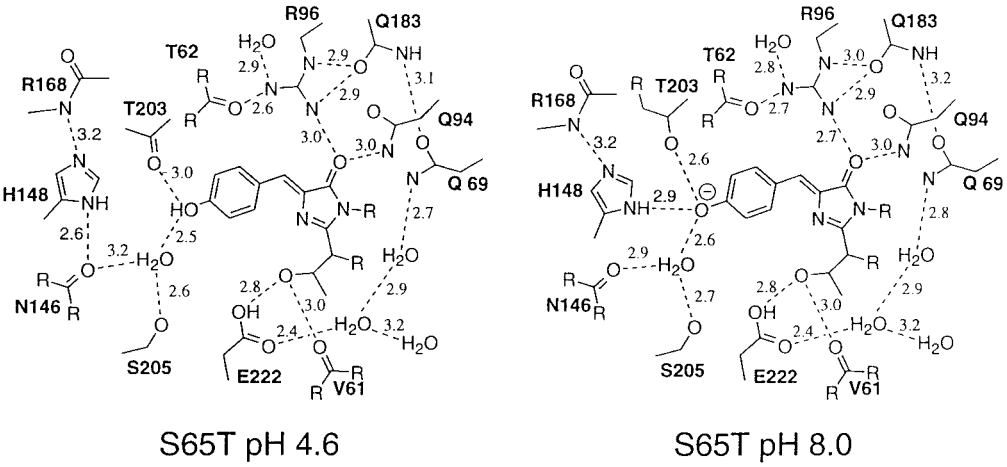

FIGURE 2: Schematic diagram showing the immediate chromophore environment of S65T at pH 4.6 and 8.0. Proposed hydrogen bonds are shown as dashed lines. Protonation states are assigned for the chromophore, His148, and Glu222 (see text).

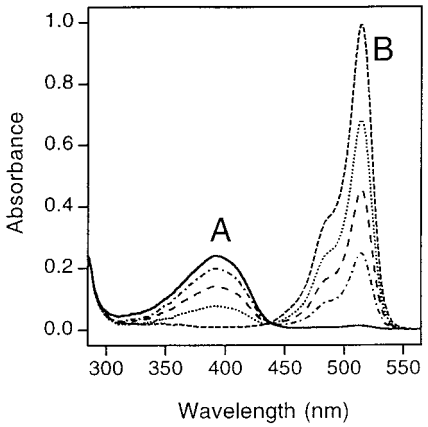

FIGURE 3: pH-dependent absorbance of YFP. Data were collected at 0.37 mg/mL protein in 75 mM buffer (CHES, Tris, phosphate, or acetate) and 140 mM NaCl. pH from top to bottom curve (band B): (- - -) 8.6, (•••) 7.2, (— —) 6.8, (-•-) 6.4, and (—) 5.0.

Table 3: Absorption and Emission Maxima of GFPs

	absorbance band		emission band[a]	
	A	B	A	B
WT GFP	395	475	460/508	504
S65T	394	489	weak	511
S65T/H148D	415	487	510	510
YFP	392	514	negligible	528
YFP H148Q	396	515	negligible	529
YFP H148G	397	512	negligible	528
YFP E222Q	402	510	negligible	525

[a] Emission band A results from excitation at the absorbance peak of band A, and emission band B results from excitation at the absorbance peak of band B.

since the side chain of Glu222 was found to make a hydrogen bond with the heterocyclic ring nitrogen of the chromophore in YFP (*7*). The protonation state of the Glu222 carboxylate should therefore be correlated to the protonation state of the chromophore ring nitrogen (Scheme 1).

All YFPs exhibit similarly red-shifted spectra. The furthest shift occurs for YFP H148Q with band B absorption at 515 nm and emission at 529 nm (Table 3). The ionization constants determined by absorbance and by fluorescence are nearly identical (Table 2), indicating that the quantum yield of fluorescence does not change with pH (*13*). In all cases,

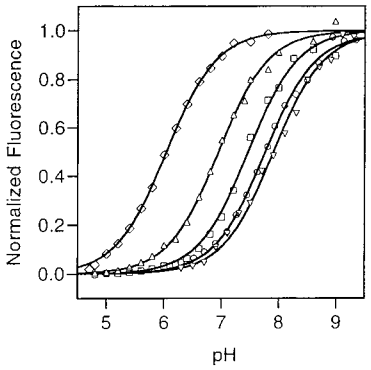

FIGURE 4: Normalized fluorescence as a function of pH. Data were collected for (from left to right) S65T (◇), YFP (△), YFP H148Q (□), S65T/H148D (○), and YFP H148G (▽). The protein solutions contained 75 mM buffer (CHES, Tris, phosphate, or acetate) and 140 mM NaCl. Excitation was carried out at the band B absorbance maximum for each variant, and emission was monitored at the fluorescence maximum for each variant (Table 2). For each case, the data points were fitted to a theoretical titration curve with one titratable group.

the absorbance intensity of the low-energy band B, as well as the emission intensity upon excitation of band B, fits well to a theoretical titration curve that describes a single titratable group (Figure 4). By fluorescence, S65T has a pK_a of 6.0, consistent with previous reports (*13*, *14*). S65T/H148D has a pK_a of 7.8 (Table 2), a shift of nearly 2 orders of magnitude in the equilibration constant for ionization, presumably due to the proximity of the negatively charged residue. Whether the introduced aspartate forms a hydrogen bond with the chromophore is as yet unknown.

The pK_a of YFP is 7.0, similar to the pK_a of 7.1 determined for a related variant that also contains the T203Y substitution (*14*). The pK_a of YFP E222Q is 7.0 as well, that of YFP H148Q is 7.5, and that of YFP H148G is 8.0 (Table 2). Though the isosbestic point is very clean for YFP and YFP E222Q (Figure 3), this is not true for the YFP H148Q and H148G variants, indicating multiple processes occurring simultaneously. The pK_as for YFP H148Q and H148G listed in Table 2 must therefore be considered estimates only. Though we have been unable to grow diffraction quality crystals of YFP H148Q, the data suggest that Gln148 may be flipped out into the solvent so that the chromophore is only partly shielded by the glutamine. Partial exposure to

exterior solvent may explain the higher pK_a of H148Q, similar to H148G where the crystal structure shows clearly that the chromophore is solvent accessible (*7*). Together, these variants display a range of pK_as between 6 and 8 (Figure 4).

Protonation State of Glu222. We propose that Glu222 is neutral at high and low pH in both S65T and YFP. In S65T, no positional changes of Glu222 were detected as a function of pH. Glu222 is involved in a hydrogen bond with the hydroxyl of Thr65 which is also hydrogen bonded to the backbone oxygen of residue 61 (Figure 2). This network suggests that Glu222 is an H-bond donor to Thr65 (*2*) and provides a rationale for the rather low pK_a of the S65T chromophore. Though the structure of YFP was determined at pH 6.9 only, the pK_as of YFP and YFP E222Q are nearly identical (Table 2), indicating that the E222Q substitution does not change the charge distribution around the chromophore, in further support of a neutral glutamic acid.

Since the presumably protonated Glu222 is directly H-bonded to the imidazolinone nitrogen of the chromophore in YFP (*7*), this nitrogen is most likely unprotonated, as suggested for S65T from the structural studies described above (Scheme 1). The pK_a of the glutamic acid is apparently perturbed by the hydrophobic environment to a higher value than in aqueous medium where it is 4.5 (*26*).

YFP E222Q appears to affect folding of the protein, since a large fraction of expressed protein precipitated during purification and less than 4% of the final purified protein was fluorescent. Upon concentration, the nonfluorescent fraction precipitated, indicating that improper folding may be preventing the generation of the chromophore.

Protonation State and Function of His148. The pK_a of His148 is most likely below 5 in both S65T and YFP. For both proteins, a clean isosbestic point is maintained throughout the entire range of titration, and the chromophore absorbance maxima do not shift (Figure 3). In both the low and high pH structures of S65T, the imidazole proton can be assigned to $N_{\delta 1}$, since this nitrogen is a hydrogen bond donor to the backbone oxygen of Asn146 at pH 4.6 and a donor to the chromophore phenolate at pH 8.0 (Figure 2). The imidazole $N_{\epsilon 1}$ is a hydrogen bond acceptor from the backbone nitrogen of Arg168 in both cases, providing a rationale for the apparently lowered pK_a of His148 as compared to an aqueous histidine (*26*).

The phenolic end of the chromophore, the proposed site of titration, is quite close to the protein surface, with His148 constituting a barrier to bulk solvent (*2, 4, 7*). However, the pH titrations show clearly that rapid and facile proton transfer occurs between the exterior solvent and the chromophore with no apparent requirement for His148 in the mechanism of titration. Rather, His148 appears to be involved in protecting the chromophore from solvent perturbations or conformational changes, on the basis of the loss of a clean isosbestic point when this residue is replaced with a glutamine or glycine in YFP.

Relative Fluorescence of the Neutral Chromophore. Excitation of the neutral chromophore (band A) leads to bright green fluorescence only in the WT protein (*27*). The variants (with the exception of S65T/H148D, see below) generally exhibit very little fluorescence upon excitation with UV light (Table 3). Under these conditions, S65T emission is less than 5% of maximal fluorescence and YFP emission is less than 0.5% of maximal fluorescence over the entire pH range of protein stability (Table 3 and Figure 5B). This loss of fluorescence upon chromophore protonation is apparently not due to a change in ground-state geometry, since the S65T chromophore is planar in both high and low pH crystal structures. On the other hand, the excited state may be able to undergo out-of-plane distortions that could result in enhanced radiationless decay. The WT chromophore appears to be embedded in a more rigid hydrogen-bonding network that may disfavor such distortions, consistent with the general rule that rigid systems tend to fluoresce (*28*).

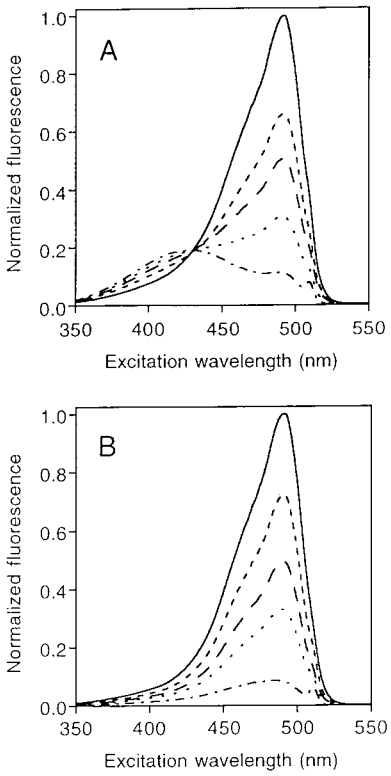

FIGURE 5: Normalized excitation scans of S65T/H148D and S65T as a function of pH. (A) S65T/H148D emission intensity monitored at 510 nm at pH (from top to bottom) (—) 9.1, (- - -) 8.1, (— —) 7.8, (•••) 7.4, and (— • —) 6.9. (B) S65T emission intensity monitored at 511 nm at pH (from top to bottom) (—) 7.0, (- - -) 6.3, (— —) 6.0, (•••) 5.7, and (— • —) 5.0. Protein concentration was 0.01 mg/mL in 75 mM buffer (CHES, Tris, phosphate, or acetate) and 140 mM NaCl.

Unexpectedly, S65T/H148D exhibits significant green fluorescence upon excitation of band A (Table 3 and Figure 5A). Maximal intensity of emission while exciting band A is approximately 20% of maximal intensity while exciting band B. Green fluorescence upon illumination at 415 nm is clearly not simply the result of band overlap with band B, as is observed for S65T (Figure 5B). Ultrafast spectroscopy on WT has shown that band A does fluoresce at 460 nm, though this blue emission decays within picoseconds and is converted to the well-known green emission because of rapid chromophore deprotonation in the excited state (*27*). Whether excited-state proton transfer occurs in S65T/H148D as well remains to be determined. It seems that band A of S65T/H148D is rendered green fluorescent by the introduction of a strongly hydrogen-bonding group near the phenolic end of the chromophore. In this model, the aspartic acid would serve not only to rigidify the π-system but also to provide a proton acceptor with appropriate pK_a for the more acidic excited state of the chromophore (*27*).

The green fluorescence of S65T/H148D upon 415 nm excitation may serve a practical application as an improved pH reporter, since the fluorescence ratio upon excitation at 487 nm and excitation at the isosbestic point (430 nm) may be sufficient to determine the pH in vivo. Such ratios greatly facilitate quantitative imaging because they cancel out variations in expression levels, cell or tissue thickness, photobleaching, and excitation intensity.

Practical Applications. One obvious advantage of the use of GFPs over other pH reporters is the capability of targeting the molecule to subcellular organelles to report pH (and changes thereof) in vivo, in real time and most importantly with spatial resolution in a fluorescence microscope. For example, one might be interested in whether some regions of the mitochodrion are more active than others in proton translocation or whether protein transport or membrane fusion requires a pH gradient across a vesicle. These GFPs may also be useful in developmental studies. For example, it has been shown that the spatial distribution of Ca^{2+} ions in the growth cones of sensory neurons has a dominant influence on neuronal development (*29*, *30*), and this has been imaged in real time (*31*). However, whether pH gradients or changes are involved as well has not yet been established. It is known that, in addition to changes in Ca^{2+} fluxes during fertilization of sea urchin eggs (*32*), there are also increases in intracellular pH (*32*), but they have not been imaged for subcellular localization or in real time. Finally, any process involving cell polarity could involve a pH gradient, such as the establishment of root/shoot polarity in pelvetia embryos (*33*). The ease of genetically manipulating GFPs, the molecule's stability, and lack of toxicity make them ideal visual indicators for such applications in vivo.

CONCLUSIONS

We provide direct crystallographic evidence that the titrating group in the GFP chromophore is the phenolic hydroxyl, with no change in the protonation state of the imidazolinone ring nitrogen. The pK_a of the chromophore heterocyclic nitrogen and the pK_a of a nearby glutamic acid, Glu222, appear to be perturbed in S65T and YFP to maintain the neutrality of these groups, in contrast to WT where Glu222 is likely to be anionic (*3*).

Engineered GFPs can be used as probes for the measurement of pH in specific cellular compartments of live tissue, as first proposed for the blue emission variant BFP (*12*). The variants presented here exhibit a range of different pK_as between 6 and 8 (Figure 5), allowing the choice of the most appropriate variant for a particular application over the pH range of 5 to 9, which includes the pH of alkaline cellular organelles such as mitochondria. The S65T/H148D mutant is somewhat reminiscent of WT in that excitation of both neutral and anionic states of the chromophore leads to green fluorescence, possibly via excited-state proton transfer.

ACKNOWLEDGMENT

We thank Dr. Roger Y. Tsien (University of California, San Diego, CA) and Dr. Christopher Doe (University of Oregon, Eugene, OR) for critical reading of the manuscript and providing helpful discussion. GFP and YFP clones were kindly provided by Dr. Roger Y. Tsien.

REFERENCES

1. Heim, R., Prasher, D. C., and Tsien, R. Y. (1994) *Proc. Natl. Acad. Sci. U.S.A. 91*, 12501−12504.
2. Ormo, M., Cubitt, A. B., Kallio, K., Gross, L. A., Tsien, R. Y., and Remington, S. J. (1996) *Science 273*, 1392−1395.
3. Brejc, K., Sixma, T. K., Kitts, P. A., Kain, S. R., Tsien, R. Y., Ormö, M., and Remington, S. J. (1997) *Proc. Natl. Acad. Sci. U.S.A. 94*, 2306−2311.
4. Yang, F., Moss, L. G., and Phillips, G. N. (1996) *Nat. Biotechnol. 14*, 1246−1251.
5. Heim, R., and Tsien, R. Y. (1996) *Curr. Biol. 6*, 178−182.
6. Heim, R., Cubitt, A. B., and Tsien, R. Y. (1995) *Nature 373*, 663−664.
7. Wachter, R. M., Elsliger, M.-A., Kallio, K., Hanson, G. T., and Remington, S. J. (1998) *Structure 6*, 1267−1277.
8. Cubitt, A. B., Heim, R., Adams, S. R., Boyd, A. E., Gross, L. A., and Tsien, R. Y. (1995) *Trends Biochem. Sci. 20*, 448−455.
9. Prasher, D. C. (1995) *Trends Genet. 11*, 320−323.
10. Gerdes, H.-H., and Kaether, C. (1996) *FEBS Lett. 389*, 44−47.
11. Tsien, R. Y. (1998) *Annu. Rev. Biochem. 67*, 509−544.
12. Wachter, R. M., Brett, A. K., Heim, R., Kallio, K., Tsien, R. Y., Boxer, S. G., and Remington, S. J. (1997) *Biochemistry 36*, 9759−9765.
13. Kneen, M., Farinas, J., Li, Y., and Verkman, A. S. (1998) *Biophys. J. 74*, 1591−1599.
14. Llopis, J., McCaffery, J. M., Miyawaki, A., Farquhar, M., and Tsien, R. Y. (1998) *Proc. Natl. Acad. Sci. U.S.A. 95*, 6803−6808.
15. Miesenbock, G., De Angelis, D. A., and Rothman, J. E. (1998) *Nature 394*, 192−195.
16. Robey, R. B., Ruiz, O., Santos, A. V. P., Ma, J., Kear, F., Wang, L.-J., Li, C.-J., Bernardo, A. A., et al. (1998) *Biochemistry 37*, 9894−9901.
17. Ward, W. W., Prentice, H. J., Roth, A. F., Cody, C. W., and Reeves, S. C. (1982) *Photochem. Photobiol. 35*, 803−808.
18. Ward, W. W., Cody, C. W., Hart, R. C., and Cormier, M. J. (1980) *Photochem. Photobiol. 31*, 611−615.
19. Niwa, H., Inouye, S., Hirano, T., Matsuno, T., Kojima, S., Kubota, M., Ohashi, M., and Tsuji, F. I. (1996) *Proc. Natl. Acad. Sci. U.S.A. 93*, 13617−13622.
20. Cormack, B. P., Valdivia, R. H., and Falkow, S. (1996) *Gene 173*, 33−38.
21. Otwinowski, Z., and Minor, W. (1997) *Methods Enzymol. 276*, 307−326.
22. Tinant, B. T., Germain, G., Declercq, J.-P., and Van Meerssche, M. (1980) *Cryst. Struct. Commun. 9*, 671−674.
23. Tronrud, D. E., Ten Eyck, L. F., and Matthews, B. W. (1987) *Acta Crystallogr., Sect. A 43*, 489−501.
24. Jones, T. A., Zou, J.-Y., Cowan, S. W., and Kjelgaard, M. (1991) *Acta Crystallogr., Sect. A 47*, 110−119.
25. Voityuk, A. A., Michel-Beyerle, M.-E., and Rosch, N. (1997) *Chem. Phys. Lett. 272*, 162−167.
26. Fersht, A. (1985) *Enzyme structure and mechanism*, W. H. Freeman and Co., New York.
27. Chattoraj, M., King, B. A., Bublitz, G. U., and Boxer, S. G. (1996) *Proc. Natl. Acad. Sci. U.S.A. 93*, 8362−8367.
28. Barltrop, J. A., and Coyle, J. D. (1978) *Principles of photochemistry*, J. W. Arrowsmith Ltd., Bristol, Great Britain.
29. Amato, A., Al-Mohanna, F., and Bolsover, S. (1996) *Brain Res. Dev. Brain Res. 92*, 101−110.
30. Obrietan, K., and van den Pol, A. (1997) *J. Neurosci. 17*, 4785−4799.
31. Gitler, D., and Spira, M. (1998) *Neuron 20*, 1123−1135.
32. Carroll, D., Albay, D., Terasaki, M., Jaffe, L., and Foltz, K. (1999) *Dev. Biol. 206*, 232−247.
33. Kropf, D., Henry, C., and Gibbon, B. (1995) *Eur. J. Cell Biol. 68*, 297−305.

BI9902182